The 2015 World Congress on
Advances in Structural Engineering and Mechanics (ASEM15)
Incheon, Korea, August 25-29, 2015

Vortex induced vibration of an inclined finite-length square cylinder

*Gang Hu[1)] K.T. Tse[2)] and K.C.S. Kwok[3), 4)]

[1), 2), 3)] *Department of Civil and Environmental Engineering, The Hong Kong University of Science and Technology, Clear Water Bay, Kowloon, Hong Kong, China.*
[4)] *Institute for Infrastructure Engineering, University of Western Sydney, Penrith, NSW, 2751, Australia.*
* *ghuaa@ust.hk*
[2)] *timkttse@ust.hk*
[3), 4)] *K.Kwok@uws.edu.au*

ABSTRACT

This study investigated the vortex-induced vibration of a slender square-section cylinder inclined from the vertical direction by a series of angles. Both aeroelastic tests and pressure measurements were performed on the cylinder with forward inclinations (inclined to the upwind direction), a vertical attitude, and backward inclinations (inclined to the downwind direction). The aeroelastic test results show that vortex-induced responses of the cylinder decrease considerably as increasing the forward inclination angle. In contrast, the effect of backward inclination on the vortex-induced vibration varied. Not all the backward inclined cylinders exhibited across-wind responses smaller than those of the vertical cylinder. The responses of the cylinder with a small backward inclination are significantly larger, whereas the cylinder with a large backward inclination exhibits lower responses than those of the vertical case. The variation in the vortex-induced vibration response with the inclination is explained by performing power spectral analyses on the pressure data on the side face over the cylinder span, which reveals local vortex shedding characteristics.

Keywords: vortex-induced vibration; inclined cylinder; aeroelastic test; vortex pair

---

[1)] PhD Student
[2)] Assistant Professor
[3)] Emeritus Professor, [4)] Professor

1. Introduction

Vortex-induced vibrations of a cylinder occur when the vortex shedding frequency is close to one of the natural frequencies of the cylinder. The cylinder undergoing vortex-induced vibration is able to oscillate at high amplitudes. The vortex-induced vibration is a self-excited phenomenon and it can lead to the fatigue failure of the structure. Thus, it has been the topic of extensive studies(e.g.Feng 1968; Hartlen and Currie 1970; Hayashida and Iwasa 1990; Kawai 1992; Williamson and Govardhan 2004; Amandolèse and Hémon 2010).

The majority of previous studies were devoted to studying vortex-induced vibrations of structures with their principal axes perpendicular to the oncoming flow, for instance, tall buildings and towers subject to a boundary layer flow. However, some slender structures in reality, such as the pylons of the Alamillo Bridge in Spain (see Fig. 1) and the HongShan Bridge in China, are inclined. Predictably, the inclination of the slender structure has a significant impact on its vortex-induced vibration.

Fig. 1The Alamillo Bridge in Spain.

Investigations to evaluate the influence of the inclination on the vortex-induced vibration of slender structures have been made by using both experimental and numerical approaches.Nakagawa et al. (1998) adopted free oscillation experiments to study the vortex-induced vibration of circular cylinders at different yaw angles and found that the response characteristics of the yawed cylinder follow the cosine law, at least up to a yaw angle of 45°. Franzini et al. (2009) investigated vortex-induced vibrations of inclined cylinders by aeroelastic tests. The cylinders with circular and elliptical cross-sections were tested. More recently, Franzini et al. (2013)evaluated the vortex-induced vibration for circular cylinders

with both upstream and downstream inclinations by using an aeroelastic model as well. Differences in the oscillation amplitudes were observed between the upstream and downstream inclinations, which were associated with the asymmetric end conditions. Meanwhile, the Independent Principle (equivalent to the cosine law) was also assessed, the validity of which is up to a yaw angle of 20°. Another study about the vortex-induced vibrations of an inclined circular cylinder was conducted by Jain and Modarres-Sadeghi (2013). Their results show that as the inclination angle was progressively increased, the lock-in range started at a higher reduced velocity.

The above studies have investigated the vortex-induced vibration of inclined circular cylinders comprehensively. However, to the authors' knowledge, the vortex-induced behavior of an inclined square-section cylinder has never been systematically investigated, although this type of cylinder has been found in the form of inclined pylons, architectural sculptures, and even iconic tall buildings (e.g. the Gate of Europe located in Madrid, Spain).

The objective of the present study is to investigate the effects of inclinations on the vortex-induced vibrations of a square-section cylinder by using aeroelastic tests to measure its across-wind responses directly in a wind tunnel. Pressure measurements on a static cylinder with dimensions identical to the aeroelastic model were also conducted to acquire the pressure distributions on the surface of the cylinder. The pressure data were used to reveal vortex-shedding characteristics by spectral analyses. The results will be examined to advance the understanding of the influences of inclinations on the vortex-induced vibrations were clarified.

1 Experimental setup

1.1 Wind tunnel facility and flow field

Aeroelastic tests and pressure measurements were carried out in the high-speedsection (3×2 m^2) of the CLP Power Wind/Wave Tunnel Facility at the Hong Kong University of Science and Technology. The tests were performed under a turbulent flow generated by using roughness elements and spires upstream of the test section. Instantaneous wind speeds were measured to determine the mean wind speed and turbulence intensity profiles by using a hot-wire anemometer installed at different heights in the test section where the model was positioned. The target mean wind speed and turbulence intensity profiles were determined according to the specifications corresponding to an open terrain (i.e. Category 2) in the AS/NZS 1170.2:2002 (Standards Australia/Standards New Zealand 2002). Comparisons of the measured mean wind speed and turbulence intensity profiles with the target profiles as shown in Fig. 2 indicate the reliability of the test condition.

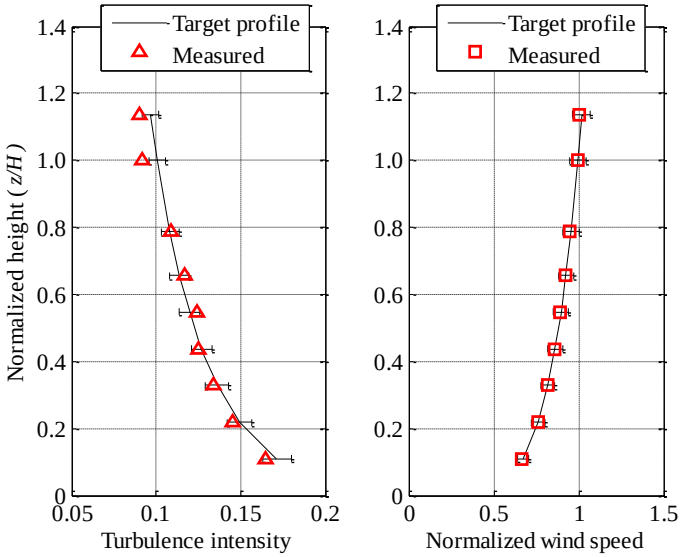

Fig. 2Turbulent wind flow fieldadopted in the wind tunnel tests.

1.2 Aeroelastic tests

To investigate the influence of the inclinations on vortex-induced vibration of slender cylinders, a series of aeroelastic tests were carried out on a square-section cylinder inclined from the vertical direction by a range of angles to acquire the across-wind responses directly. The tested model was a slender square-section tower whose height-to-width ratio is 18. For an adopted length scale of 1:250, the dimensions of the prototype were 12.7m×12.7m×228.6m.The model was made of square aluminum hollow cylinder with width$D$= 5.08 cm (2 inches) and height H= 91.44 cm (36 inches). The blockage ratio of the model in the wind tunnel was about 0.8% which is well below the critical value of 5% (Holmes 2001).

The model was pivoted at the base by a gimbal, allowing for one sway mode of vibration in the transverse direction, as shown in Fig. 3. The model mass was adjusted to represent an equivalent density ρ_s= 250 kg/m^3, and the model stiffness was provided by two horizontal springs underneath the wind tunnel turntable. The natural frequency of the model was approximately f_n= 8 Hz, which simulated a prototype structure with a natural frequency of 0.32 Hz. The structural damping ratio was approximately 0.7% of critical damping, which was achieved by immersing an aluminum plate into an oil bath. The cylinder was adjusted manually to set the inclination angle α according to the values listed in Table 1.While positive values represent forward inclinations, negative values denote backward inclinations. The inclination angle of 0° implies the vertically erected cylinder. A sketch illustrating the inclination geometry is presented in Fig. 4.All the aeroelastic tests were performed at a wind incidence angle β = 0°. Strain gauge bridges were

used to measure the tip displacement. Before each individual aeroelastic test, a free vibration test was conducted to confirm the fundamental frequency and the damping ratio.

Table 1Inclination angles of the cylinder for the wind tunnel tests

Inclination angle (°)	0	±5	±10	±15	±20	±30

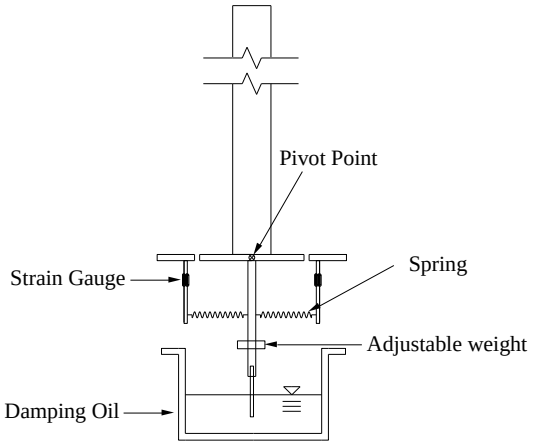

Fig. 3 Schematic of the aeroelastic model used in the wind tunnel tests.

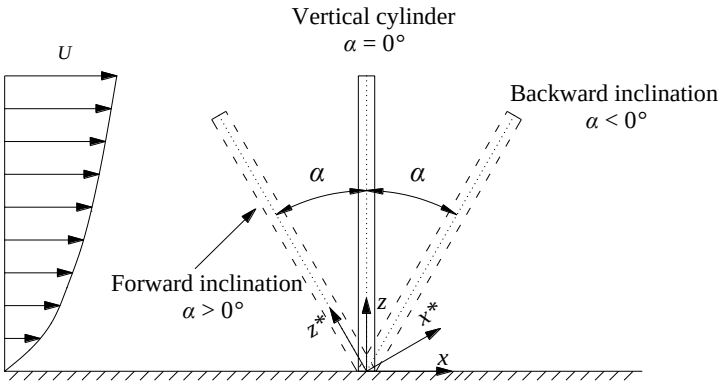

Fig. 4 Illustration of tested three different types of cylinders: the forward inclined cylinder, the vertical cylinder, and the backward inclined cylinder. $\alpha$is the angle of inclination: a positive value represents the forward inclination while a negative one denotes the backward inclination.

1.3 Pressure measurements

A static model with the same dimension of the aeroelastic model was used to perform the pressure tests, as shown in Fig. 5. Pressures acting on the surfaces of the rigid model were collected through asynchronous multi-pressure sensing system (SMPSS), and the total number of pressure taps was220. The measurements were taken by using high-speed scanning pressure equipment and 14 electronic pressure scanners. The 220 pressure taps were distributed among 11 levels over the span, 20 taps on each level, and 5 taps for each side on each level, as shown in Fig. 5. The sampling frequency and duration were 400 Hz and 120 seconds respectively. The reference point was taken to be the top of the vertical cylinder, and the corresponding mean velocity, i.e., V_{ref}, was kept at a constant of approximately 12 m/s regardless of the inclination angle. The test Reynolds number *Re*based on the width *D* and the reference velocity V_{ref}, was 4×10^4. More details of the pressure tests can be found in Hu et al. (2015).

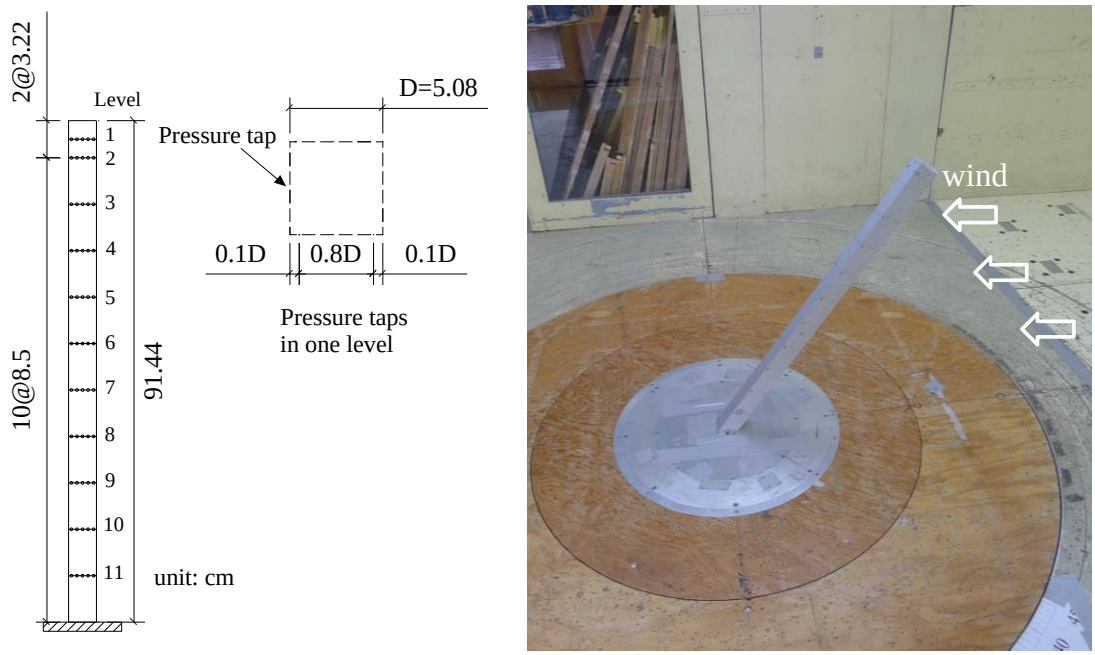

(a) (b)

Fig. 5A model for wind tunnel pressure measurements: (a) the tested model dimensions and the distribution of pressure taps, (b) a square-section cylinder with a forward inclination angle in the wind tunnel.

2 Across-wind response amplitudes from aeroelastic tests

Normalized root mean square (RMS) of tip across-wind displacements (i.e. σ_y/D) of the cylinder with different inclinations wascomputed to evaluate the influence

of the inclination on the vortex-induced vibration. The normalized response of forward inclined cylinders ($\alpha > 0°$) compared with the vertical cylinder ($\alpha = 0°$) are presented in Fig. 6. The corresponding responses of backward inclination cases are shown in Fig. 7. In addition, the across-wind response corresponding to a vertical square-section cylinder with an aspect ratio of 18 at a reduced wind speed V_{red} ($=V_{ref}/fD$)of 16 (Kwok and Melbourne 1980) is included to evaluate the reliability of the present aeroelastic tests. The comparison indicates that the present test rseults agree well with results of a similar testwhen considering the differences in the damping ratio and the turbulence intensity between the two studies.

As shown in Fig. 6, the across-wind response of the vertical cylinder increase nearly linearly with reduced wind speed. The ordinary vortex-induced peak is not observed, which is similar to the observation in the studies of Parkinson and Wawzonek (1981) and Hu et al. (2015). The absence of the peak is due to an interaction between vortex-induced vibration and galloping, which occurs as the galloping onset wind speed is close to the Karman-vortex resonance speed (Mannini et al. 2014). As the forward inclination is increased, the response decreases progressively. Unlike the vertical case, at $V_{red} = 11$, the vortex-induced peak appears at the range of $5° \leq \alpha \leq 15°$. The presence of the peak at $V_{red} = 11$ at the range of $5° \leq \alpha \leq 15°$ may be due to a separation of the vortex-induced vibration from galloping. According to the observation in Hu et al. (2015), the galloping onset wind speed is significantly increased at $\alpha = 5°$and galloping is absent as $\alpha \geq 10°$. Therefore, it is anticipated that there is little or no interaction between vortex-induced vibration and galloping at $V_{red} = 11$ for the inclination of $5° \leq \alpha \leq 15°$. In addition, the peak broadens as $\alpha$is further increased and it finally disappears as $\alpha \geq 20°$. This suggests that the vortex-induced vibrations are entirely suppressed in the case with such large forward inclination. The resultant responses are possibly caused by turbulence buffeting of the oncoming flow, which is verified in the following section.

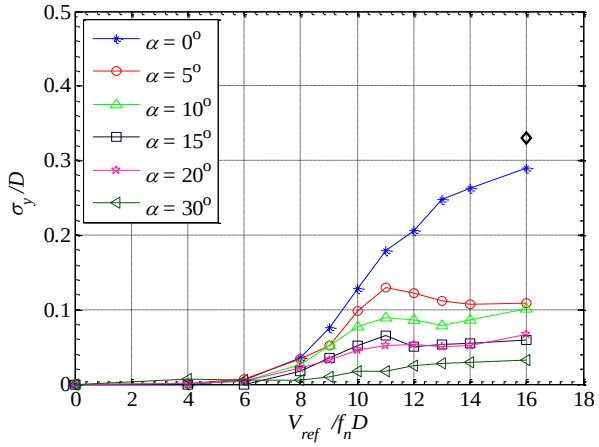

Fig. 6 Across-wind responses of forward inclined cylinders compared with the vertical cylinder. ◊: transverse amplitude of a vertical cylinder with *H/D*= 18, damping ratio of 0.64%, and turbulence intensity of 9%(Kwok and Melbourne, 1980).

For the backward inclination as shown in Fig. 7, its influence on the vortex-induced vibration varies compared with that for the forward inclination. The backward inclination does not reduce the across-wind response monotonously. Increasing the backward inclination from α= 0° first raises the response and then reduces it. In detail, the cylinders with α= -5° and -10° have larger responses than the vertical cylinder has; the cylinder with α= -5° exhibits the largest responses. When the backward inclination angle is greater than 10° (i.e. α= -15°, -20° and -30°), the responses are lower than that of the vertical case. Meanwhile, at this range of the backward inclination, the response decreases with an increase in the backward inclination. Compared with the forward inclination, the reductions in the across-wind response caused by the backward inclination are less significant. In addition, the ordinary vortex-induced peak at V_{red} = 11 is completely absentfor all the backward inclinationcases. Similar to α= 0°, the absence of the peaks for the cases except α= -30° is attributable to the interaction between vortex-induced vibration and galloping as well.Indeed, the galloping oscillations at α= -5° and -10° are more intense than that at α= 0° and the galloping oscillations at α= -15° and -20° are generally comparable to that at α= 0°, as reported by Hu et al. (2015). Whilst, forα= -30°, the disappearance of the response peak may be associated with the supression of the Karman vortex shedding.

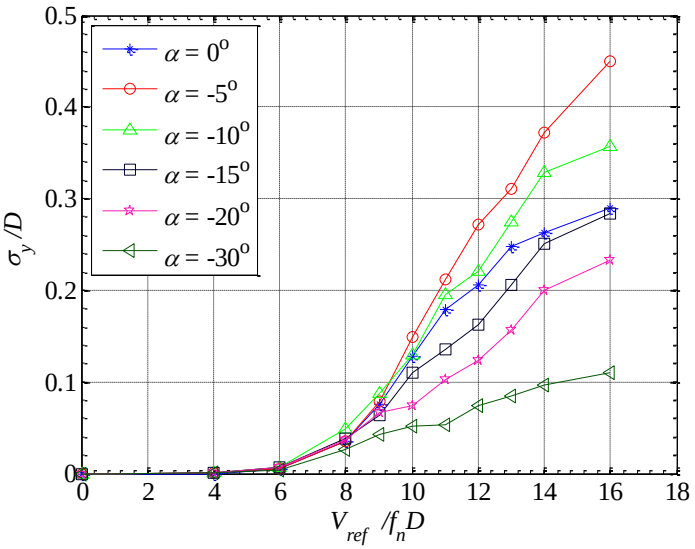

Fig. 7 Across-wind responses of backward inclined cylinders compared with the vertical cylinder.

3 Discussions

3.1 Power spectra of across-wind responses

The power spectra of the across-wind response of the cylinder with different inclinations at V_{red}=11, where the vortex-induced peak locates in the response against wind speed curve (see Fig. 6), are shown in Fig. 8. For the vertical case (α = 0°), there is a pronounced peak at f_v/f_n =1, which indicates that the Karman vortex shedding frequency f_v coincides with the structural natural frequency f_n. As the forward inclination is increased, the peak value gradually decreases. At α = 30°, the peak is significantly reduced. The energy transferred to the higher frequency range, which induces the considerable reduction in the responses of the cylinder as shown in Fig. 6. In terms of the spectrum of the response, it can be inferred that the response of the cylinder with α = 30° at V_{red}=11 is largely attributed to buffeting that caused by turbulence of the oncoming flow, which results in the absence of the vortex-induced peak in Fig. 6.

For the backward inclination, the spectrum for α = -5° exhibits a slightly sharper peak than that for α = 0° at V_{red}=11. The sharper peak implies that the Karman vortex shedding energy is more concentrated for α = -5°, causing a higher response than that for α = 0°. For α = -15°, the peak value is reduced and lower than that for α = 0°. Increasing the backward inclination to α = -30° further reduces the Karman vortex shedding energy at V_{red}=11, which results in the reduction in the across-wind response. In addition, compared with the forward

inclination cases, the spectra of the backward inclination cases show higher peak values at V_{red}=11, which echoes that the backward inclined cylinder exhibits greater responses than the corresponding forward inclined cylinder does as shown in Fig. 6 and Fig. 7.

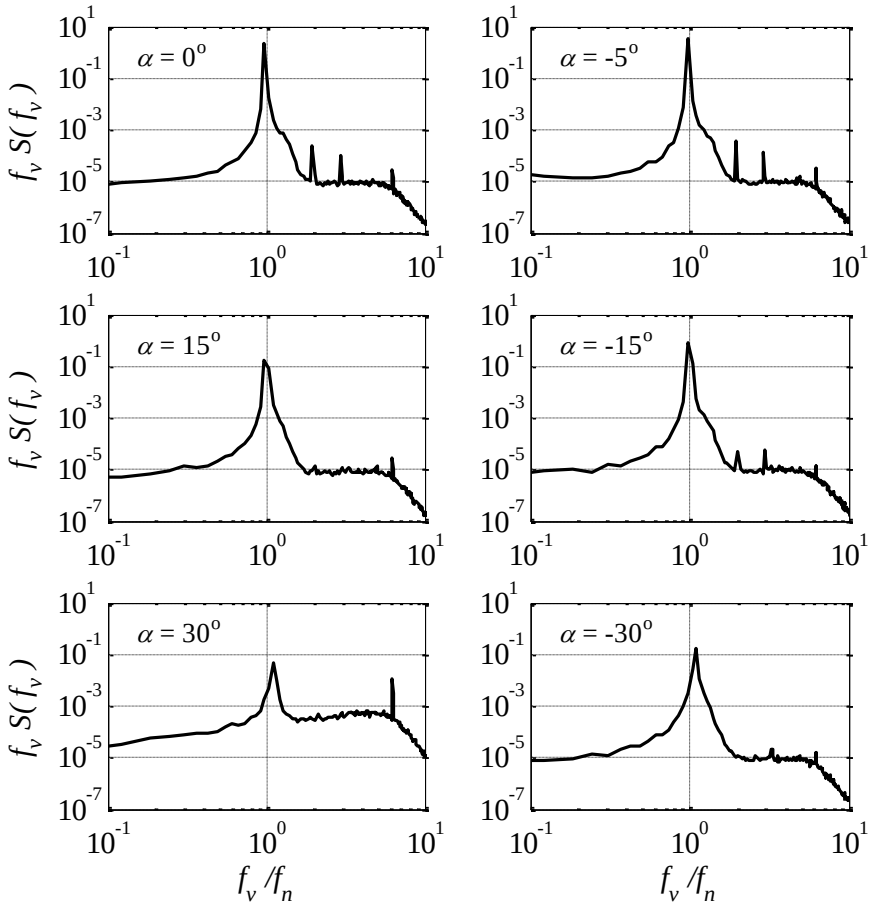

Fig. 8 Power spectra of across-wind responses of the cylinders at V_{red} =11.

3.2 Spectrum analyses of pressure on the side face

To understand the variation in the spectra induced by the inclinations as shown in Fig. 8, spectrum analyses of pressure coefficients at the middle pressure taps on the side face of the static model over the cylinder height were performed, by which local features of vortex shedding are revealed.

As shown in Fig. 9 (a), the vortex shedding energy for the vertical cylinder in general concentrates at the Strouhal frequency of 0.11, which is identical to the value reported by Wang and Zhou (2009). Sharp peaks can be observed in the

spectra over the whole height. Compared with the vortex shedding frequency for the mid-span of the vertical cylinder, slight decreases occur near the two ends, which are thought to be a result of the presence of the free end vortex pair and the base vortex pair (Sumner et al. 2004; Hu et al. 2015). In other words, the separated shear layers that roll up at the leading edge near the free end and the base interact with the free end vortex pair and the base vortex pair respectively. The interactions delay the development of the vortex shedding and hence reduce its frequency.

As the forward inclination is increased, the peak values of the spectra over the cylinder height are considerably reduced as shown in Fig. 9 (b) and (c). Furthermore, the reductions near the free end are quite remarkable compared with the other heights. Meanwhile, the vortex shedding frequencies near the free end also reduce significantly. That is to say, the Karman vortex shedding near the free end of the forward inclined cylinder is suppressed significantly. The suppression of the Karman vortex shedding is attributed to the free end vortex pair as reported by Hu et al. (2015). In their study, the large eddy simulation results show that the free end vortex pair extends over most of the span of the forward inclined cylinder. The “extended free end vortex pair” serves to interfere with the Karman vortex shedding from the sides of the cylinder. The interference of the two types of vortex structures reduces the Karman vortex shedding energy and generates cellular shedding structures (Ayoub and Karamcheti 1982). The cellular structures have lower shedding frequencies than the Karman vortex shedding frequency, which contributes to the reduction in the shedding frequency in the forward inclination cases.

On the contrary, the suppression of the Karman vortex shedding near the base of the backward inclined cylinder is more evident than that near the free end. The spectral peaks near the base are widened and shifted to the lower frequency regions, which can be ascribed to the “extended base vortex pair” as reported in Hu et al. (2015). The “extended base vortex pair” in the wake of the backward inclined cylinder behaves like the “extended free end vortex pair” of the forward inclined cylinder, and interacts with the Karman vortex. This interaction delays the development of the Karman vortex shedding and hence decreases the corresponding energy. Meanwhile, the cellular vortex with low shedding frequencies is generated, which causes the reduction in the vortex shedding frequency. However, it is worthwhile noting that the peak values near the free end of the backward inclined cylinder with small backward inclinations (i.e. α = -5° and -15°), especially for α = -5°, are higher than those of the vertical cylinder. Meanwhile, for the other heights except the part near the free end of the cylinder with α = -5°, the peak values are not lower than those for the corresponding heights of the vertical cylinder. As a consequence, the overall Karman vortex shedding energy for α = -5° is greater than the energy for α = 0°, which results in the higher peak value in the response spectrum (see Fig. 8) and larger responses

for α = -5° than α = 0° (see Fig. 7). Additionally, although the peak values near the free end for α = -15° is higher than those for α = 0°, the overall vortex shedding energy is still lower than that for α = 0° due to the suppression in the vortex shedding for the other heights for α = -15°. As a result, the spectrum of the across-wind response for α = -15° has a slightly lower peak than that of the vertical cylinder, and therefore the cylinder with α = -15° has a lower across-wind response. The higher peak values near the free end of the backward inclined cylinder with small backward inclinations than those of the vertical cylinder can be attributed to the absence of the free end vortex pair induced by the "extended base vortex pair" (Hu et al. 2015).

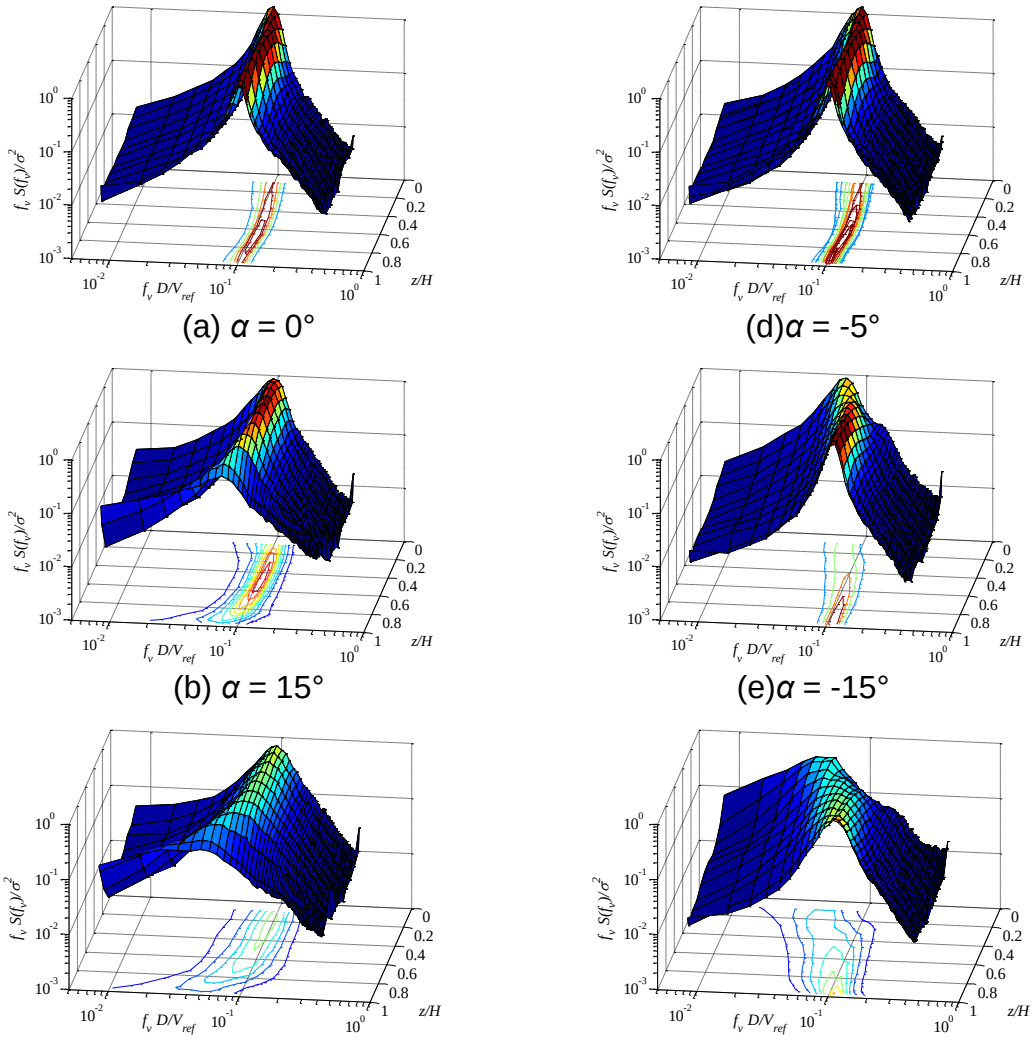

(a) α = 0° (d)α = -5°

(b) α = 15° (e)α = -15°

(c) α = 30° (f) α = -30°

Fig. 9 Power spectra of pressures on the side face of the cylinders

4 Conclusions

This study investigated the vortex-induced vibration of a slender square-section cylinder inclined from the vertical direction by aeroelastic tests and pressure tests in a wind tunnel. Significant effects on the vortex-induced vibration resulting from the inclinations have been observed. Furthermore, the mechanisms of the effects have been clarified by the spectrum analyses of the pressure data.

According to the aeroelastic tests, the across-wind responses of the cylinder decrease progressively as the forward inclination is increased. In contrast, the influence of the backward inclination on the vortex-induced vibration varies. The backward inclination does not reduce the across-wind response monotonously. The cylinders with α= -5° and -10° have larger responses than the vertical cylinder. For the cases with α= -15°, -20° and -30°, the responses are lower than that of the vertical case. Compared with the forward inclination, the reductions in the across-wind response caused by the backward inclination are less significant.

As the forward inclination is increased, the peak value of the power spectra of the across-wind response gradually decreases. For the large forward inclination (i.e.α = 30°), the peak is significantly reduced and the energy transfers to the higher frequency range, which induces the considerable reduction in the responses of the cylinder. Therefore, it can be inferred that the response of the cylinder with α = 30° at V_{red} =11 is largely attributed to buffeting that caused by turbulence of the oncoming flow. For the backward inclination, the spectrum of the across-wind response for α = -5° exhibits a slightly sharper peak than that for α = 0° at V_{red} =11. For α = -15° and -30°, the peak value is reduced and lower than that for α = 0°, which results in the reduction in the across-wind response. Compared with the forward inclination cases, the spectra of the backward inclination cases show greater peak values, which echoes that the reductions in the across-wind responses caused by the backward inclination are less significant than by the forward inclination.

Local features of vortex shedding are revealed by spectral analyses of pressure coefficients at the middle pressure taps on the side face of the static model over the cylinder height. The peak values of the spectra over the cylinder height are considerably reduced by the forward inclination. Furthermore, the reductions near the free end are quite remarkable compared with the other heights. Meanwhile, the vortex shedding frequencies near the free end are also reduced significantly. The suppression of the Karman vortex shedding is attributed to the “extended free end vortex pair” in the wake of forward inclined cylinders. The “extended free end vortex pair” serves to interfere with the Karman vortex and to reduce the Karman vortex shedding energy and frequencies.

Conversely, the suppression of the Karman vortex shedding near the base of the backward inclined cylinder is more evident than that near the free end. The widened spectral peaks near the base are ascribed to the “extended base vortex

pair". The "extended base vortex pair" in the wake behaves like the "extended free end vortex pair" of the forward inclined cylinder. However, the peak values near the free end of the backward inclined cylinder with small backward inclinations (i.e. α = -5° and -15°), especially for α = -5°, are higher than those of the vertical cylinder. The overall Karman vortex shedding energy for α = -5° is greater than the energy for α = 0°, which results in larger responses for α = -5° than for α = 0°. The higher peak value for the case with small backward inclination can be ascribed to the absence of the free end vortex pair caused by the "extended base vortex pair".

Acknowledgments

The authors appreciate the use of the testing facility at, as well as technical assistance provided by, the CLP Power Wind/Wave Tunnel Facility at The Hong Kong University of Science and Technology.

References

Amandolèse, X. and Hémon, P. (2010), "Vortex-induced vibration of a square cylinder in wind tunnel", *Comptes Rendus Mécanique*. **338**(1), 12-17.

Ayoub, A. and Karamcheti, K. (1982), "An experiment on the flow past a finite circular cylinder at high subcritical and supercritical Reynolds numbers", *Journal of Fluid Mechanics*. **118** 1-26.

Feng, C.C. (1968), "The measurement of vortex induced effects in flow past stationary and oscillating circular and d-section cylinders", the Degree of M.A. Sc., The University of British Columbia, Vancouver, Canada.

Franzini, G., Gonçalves, R., Meneghini, J. and Fujarra, A. (2013), "One and two degrees-of-freedom Vortex-Induced Vibration experiments with yawed cylinders", *Journal of Fluids and Structures*. **42** 401-420.

Franzini, G.R., Fujarra, A.L.C., Meneghini, J.R., Korkischko, I. and Franciss, R. (2009), "Experimental investigation of Vortex-Induced Vibration on rigid, smooth and inclined cylinders", *Journal of Fluids and Structures*. **25**(4), 742-750.

Hartlen, R.T. and Currie, I.G. (1970), "Lift-oscillator model of vortex-induced vibration", *Journal of the Engineering Mechanics Division*. **96**(5), 577-591.

Hayashida, H. and Iwasa, Y. (1990), "Aerodynamic shape effects of tall building for vortex induced vibration", *Journal of Wind Engineering and Industrial Aerodynamics*. **33**(1), 237-242.

Holmes, J.D. (2001), *Wind loading of structures*, Taylor & Francis

Hu, G., Tse, K.T. and Kwok, K.C.S. (2015), "Galloping of forward and backward inclined slender square cylinders", *Journal of Wind Engineering and Industrial Aerodynamics*. Accepted.

Hu, G., Tse, K.T., Kwok, K.C.S. and Zhang, Y. (2015), "Large eddy simulation of flow around inclined finite square cylinders", *Journal of Wind Engineering and Industrial Aerodynamics*. Under review.

Jain, A. and Modarres-Sadeghi, Y. (2013), "Vortex-induced vibrations of a flexibly-mounted inclined cylinder", *Journal of Fluids and Structures*. **43**(0), 28-40.

Kawai, H. (1992), "Vortex induced vibration of tall buildings", *Journal of Wind Engineering and Industrial Aerodynamics*. **41**(1-3), 117-128.

Kwok, K.C.S. and Melbourne, W.H. (1980), "Freestream turbulence effects on galloping", *Journal of the Engineering Mechanics Division*. **106**(2), 273-288.

Mannini, C., Marra, A.M. and Bartoli, G. (2014), "VIV–galloping instability of rectangular cylinders: Review and new experiments", *Journal of Wind Engineering and Industrial Aerodynamics*. **132**(0), 109-124.

Nakagawa, K., Kishida, K. and Igarashi, K. (1998), "Vortex-induced oscillation and lift of yawed circular cylinders in cross-flow", *Journal of Fluids and Structures*. **12**(6), 759-777.

Parkinson, G.V. and Wawzonek, M.A. (1981), "Some Considerations of Combined Effects of Galloping and Vortex Resonance", *Journal of Wind Engineering and Industrial Aerodynamics*. **8**(1-2), 135-143.

Standards Australia/Standards New Zealand (2002), *Structural Design-General Requirements and Design Actions*,

Sumner, D., Heseltine, J.L. and Dansereau, O.J.P. (2004), "Wake structure of a finite circular cylinder of small aspect ratio", *Experiments in Fluids*. **37**(5), 720-730.

Wang, H.F. and Zhou, Y. (2009), "The finite-length square cylinder near wake", *Journal of Fluid Mechanics*. **638**(1), 453-490.

Williamson, C. and Govardhan, R. (2004), "Vortex-induced vibrations", *Annu. Rev. Fluid Mech.*, **36** 413-455.